University of Bath

Alternative formats

If you require this document in an alternative format, please contact:
openaccess@bath.ac.uk

Resistive superconducting fault current limiter AC loss measurements and analysis

Xiaoze Pei, Xianwu Zeng, Alexander C. Smith, *Senior Member, IEEE,* and Daniel Malkin

Abstract—**Resistive superconducting fault current limiters (SFCL's) offer the advantages of low weight and compact structure. Multi-strand Magnesium Diboride (MgB_2) wire can be used in SFCL coil design to increase the transport current capacity. A monofilament 0.36 mm MgB_2 wire with a stainless steel sheath was used to build three SFCL coils with 3 strands, 16 (9+7) strands and 50 (28+22) strands of the MgB_2 wire.**

The quench current level and AC losses in the MgB_2 wire are critical design parameters for a resistive SFCL. The experimental results showed the measured quench current densities reduced as the strand number increased and the AC losses increased as the strand number increased. An axisymmetric 2D finite element (FE) model therefore was built to analyze the current distribution and the AC losses in the coil. The multi-stranded coil FE model showed that proximity effect can modify the current distribution in the strands. This not only reduces the current carrying ability, but also increases the AC losses non-linearly. The FE model confirmed the issues highlighted by the experimental testing. Finally a winding method for multi-strand coil has been proposed to reduce the impact of these effects.

Index Terms—**AC losses, FE model, MgB_2, Multi-strand superconductors, SFCL.**

I. INTRODUCTION

RESISTIVE superconducting fault current limiters (SFCL's) offer the advantages of low weight and compact structure. Magnesium Diboride (MgB_2) in simple round wire form has shown potential in resistive SFCL's [1-5]. Multi-strand MgB_2 wire can be used in SFCL coil design to increase the transport current capacity [4, 6]. The quench current level and AC losses in the superconducting wire are critical design parameters for a resistive SFCL. Resistive SFCLs are required to carry the transport current continuously without quench; the quench current level therefore has to be higher than the maximum normal operating current. It is also important to measure the AC losses in the superconducting wire and build a reliable model to estimate the AC losses at the design stage to optimize the cooling system [7, 8].

A monofilament 0.36 mm MgB_2 wire using a stainless steel sheath was developed by Hyper Tech and used to build three

SFCL coils with 3 strands, 16 (9+7) strands and 50 (28+22) strands of the MgB_2 wire. The paper will report on the experimental results from the multi-strand MgB_2 coils used as resistive SFCL's. The experimental results showed the measured quench current densities reduced as the strand number increased and the AC losses increased as the strand number increased.

An axisymmetric 2D finite element (FE) model was built to analyze the current distribution and the AC losses in the coil. The FE model produced very similar losses in the single strand MgB_2 to the Norris analytical model. The FE model extended to multi-stranded coils shows that proximity effects can modify the current distribution in the strands. This not only reduces the current carrying ability, but also increases the AC losses non-linearly. The FE models confirmed the issues highlighted by the experimental testing. A winding method for multi-strand wire has been proposed to reduce the impact of these effects. The paper will also include a detailed analysis of the results and the implications for the practical design of commercial SFCL's.

II. EXPERIMENTAL SETUP

A. SFCL coils

A monofilament MgB_2 wire was used to fabricate the SFCL coils. The diameter of each individual wire was 0.36 mm. Stainless steel is deliberately chosen as the sheath material for the wire to meet the requirements for application as a resistive SFCL. Three prototype SFCL coils with 3 strands, 16 (9+7) strands and 50 (28+22) strands of the MgB_2 wire were built and shown in Fig. 1. The wire strands were transposed into a braid configuration during the manufacture process to equalize the impedance of each parallel wire path.

The diameter of the alumina former was 200 mm. All of the coils were designed to cancel the main solenoidal field along the axis of the coil. Fig. 1 (a) is an interleaved 3-strand series-connected coil and each winding was made of three and half turns. Fig. 2 presents a section of the 3-strand coil of 0.36 mm wire, the twist pitch was 12 mm. Fig. 1 (b) shows two coils connected in anti-parallel, one coil formed 9 strands and the second coil form 7 strands: both coils had ten and three-quarter turns. The inner 7-strand winding was wound clockwise on the former. The outer 9-strand winding was sheathed with S-glass insulation and then wound counterclockwise [6]. Each winding was fabricated using a two-stage process: the 9-strand coil was formed by twisting 3 strands with a pitch of 27-30 mm and then 3 groups of 3

strands twisted with a pitch of 32-34 mm. Fig. 1 (c) is a pair of anti-parallel connected coils similar to Fig. 1 (b) except that there were 28 and 22 MgB$_2$ wire strand coils in parallel. In this case, a three-stage twisting process was used: the 28-strand coil was formed 2×9-strand wire group and 1×10-strand wire group twisted with a pitch of 37-39 mm; and the 22-strand coil formed from 2×7-strand wire group and 1×8-strand wire group twisted with a pitch of 37-39 mm. This coil has different strand number to ensure the quench occurred in the lower strand number coils.
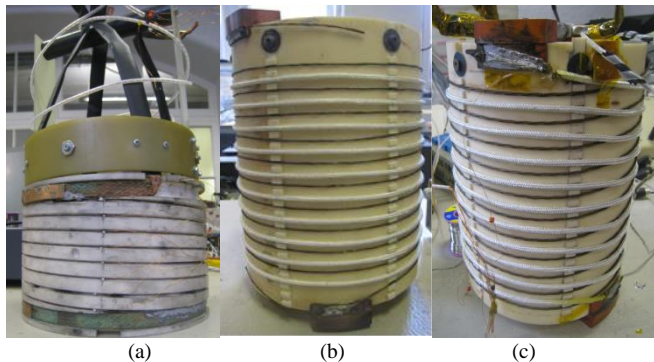

| (a) | (b) | (c) |

Fig. 2. SFCL coils: (a) 3-strand coil; (b) 16-strand (9+7) coil; (c) 50-strand (28+22) coil

Fig. 2. 3-strand wire braid

B. Test circuits

Fig. 3 shows a controllable high current supply, which was used to test the operation of these SFCL coils at the operation frequency of 50 Hz [6]. Different prospective fault current levels were achieved by adjusting the set point of the variable transformer. PC based LabVIEW system controlled the number of AC cycles supplied to the test coil and recorded voltage and current signals during testing. Fig. 4 presents the AC loss measurement circuit [9]. A 50 Hz sinusoidal signal was generated using the network analyzer and then amplified using a power amplifier. In order to increase the current level, a voltage step-down transformer was also used. The voltage and current signals were measured by the precision oscilloscope and network analyzer.
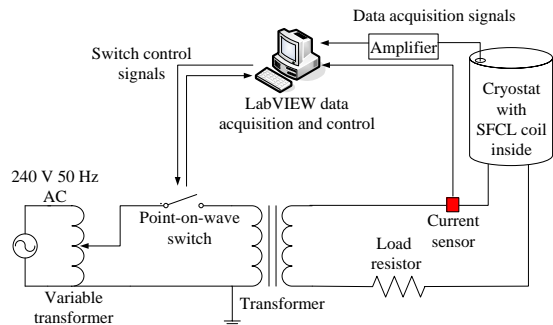

Fig. 3. High current test circuit schematic [6]

The SFCL coils were tested in a commercial cryostat which could operate from 20 K to 80 K. The test coil was placed in the copper containment vessel inside the cryostat and then filled with liquid nitrogen. Conduction cooling using a commercial Gifford-McMahon (GM) cryocooler and an internal heater with a PI controller set the temperature on the test coil.
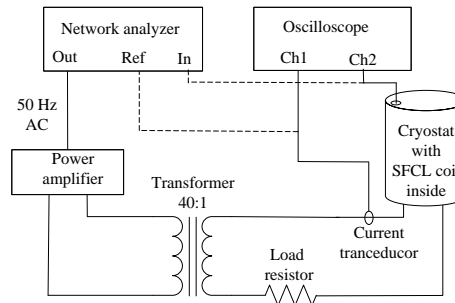

Fig. 4. AC loss measurement circuit schematic [9]

III. EXPERIMENTAL RESULTS AND DISCUSSION

A. Quench current density

The high current test circuit, as shown in Fig. 3, was used to test the quench current level of the SFCL coil. The prospective fault current level was gradually increased by manually adjusting the voltage set point of the variable transformer until the coil quenches. The prospective fault current is defined as the estimated fault current if the superconductor does not quench and is calculated based on the coil in the superconducting state with negligible impedance. Fig. 5 shows the current and voltage response for the 3-strand coil at 25 K with a prospective fault current of 250 A. It is clear that the voltage across the coil starts to increase when the current reaches 188 A and this current level is taken as the quench current for the 3-strand coil at 25 K. The peak current in the first cycle is limited from 250 A to 200 A. The quench current levels of these three SFCL coils were measured from 32 K to 23 K using the same procedure. The quench current over the area of the MgB$_2$ core gave the quench current density, which is presented in Fig. 6. Fig. 6 shows that the coils have very similar quench current densities at a temperature close to the critical temperature (32 K). The quench current densities however diverge as the temperature decreases. The 3-strand coil has the highest quench current density compared to the other two coils at every temperature point lower than 32 K. Fig. 6 shows clearly that the wires with the higher strand number have a reduced overall current density.
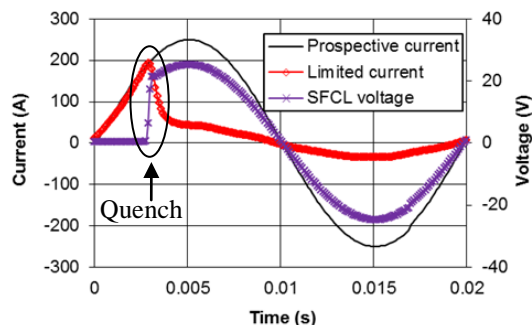

Fig. 5. Quench response of the 3-strand coil at 25 K with a prospective fault current of 250 A
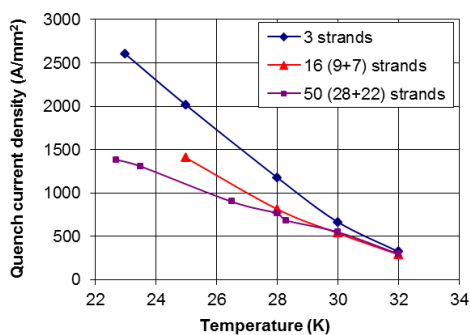
Fig. 6. Measured quench current density for different multi-stranded coils

There are three possible reasons which may explain this: firstly, the current distribution in the 16-strand coil and 50-strand coil are less uniformly distributed in the strands compared with the 3-strand coil due to differences in the proximity effects; secondly, the reduced quench current density could be related to the double/triple stage twisting process used to fabricate the 16-strand/50-strand coil putting additional stresses on the wire; thirdly, the coil was found to begin quenching at the coil ends where they were connected to the copper braids. The temperature of the copper braid is normally slightly higher than the MgB_2 coil. The copper braid incurs Joule losses when current is flowing through it, which also causes the temperature to rise. This would mean that the coil ends were slightly warmer than the coil leading to a reduction in the quench current. The higher current flowing through the copper braiding the higher strand number would mean higher Joule losses and therefore potentially a higher temperature of the coil ends.

B. AC losses

AC losses of the SFCL coils were measured using the circuit shown in Fig. 4. The current and voltage signals from the SFCL coil were input to a high sampling rate oscilloscope and a network analyzer. The oscilloscope recorded the instantaneous current and voltage signal whilst the network analyzer provided the modulus of voltage over current and phase angle. Correlation of the results from these two methods was used to assess the accuracy of the measurements.

Fig. 7 presents the measured AC losses at 25 K in the three multi-stranded coils as a function of the current density in the MgB_2. The SFCL coil was placed in a copper containment vessel during the test. The measured AC losses are made up mainly of three parts: hysteresis losses in MgB_2 wire, eddy current losses in the sheath materials and copper container, and coupling losses [8]. The hysteresis losses estimated by the Norris model follows a current cubic dependence [10]. The eddy current losses in the stainless sheath and the copper containment vessel contributed to the current squared portion. Fig. 7 shows that the variation in losses is closely proportional to current squared, which indicates that the eddy current losses in the copper containment vessel are dominating the losses. It is difficult to subtract the eddy current losses in the copper containment vessel from the total losses. Fig. 7 would indicate that the AC loss in MgB_2 wire merely contributes a small portion of the total measured losses.
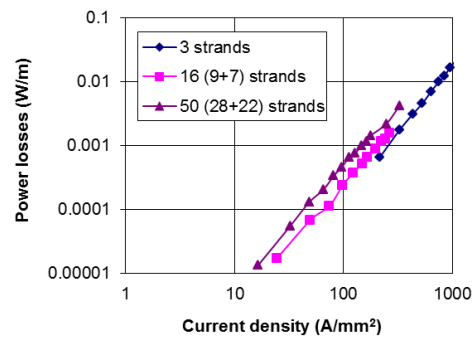

Fig. 7. Power losses in different multi-stranded coils at 25 K

The wire strands in the three coils use the same wire, so the Norris analytical model would predict the same losses per unit length per strand as a function of current density. However Fig. 7 shows that the losses are increasing as the strand number increases. This again may due to less uniformly current distributed in the 16-strand and 50-strand coil compared with the 3-strand coil.

The experimental results showed the measured quench current densities reduced as the strand number increased and the AC losses increased as the strand number increased. To fully understand the experimental results, it is important to build a model that can simulate the current distribution in the multi-strand coil and also estimate the AC losses in the MgB_2 wire.

IV. MODELLING AND SIMULATION

A commercial finite element software package Flux 2D was used to model the superconductor wire [11]. The nonlinear *E-J* power law was implemented to represent the superconducting material.

A straight round MgB_2 wire model was built initially to verify the accuracy of the Flux 2D model. The diameter of the wire was 0.36 mm and the fill factor was 25%. The critical current density of MgB_2 was assumed to be 75 kA/cm^2 at 25 K. The critical current for single wire therefore was 19.1 A and the *n*-value was set to 30. The superconducting wire was connected to an external current source to drive a peak transport current of 11.4 A, which is 60% of the wire critical current. Fig. 8 (a) shows the current distribution in the single strand wire at 0.015 second with peak negative current (system frequency of 50 Hz). Since there was no external magnetic field source, the AC loss from the single MgB_2 wire was due to self-field losses produced by the transport current only. The AC losses from Flux 2D showed good agreement with the Norris analytical model [10]. The results also confirm that the hysteresis loss is the dominant loss for a single superconducting wire and the stainless steel sheath loss is almost negligible in comparison at the system frequency of 50 Hz.

To meet the higher operating current levels needed for distribution applications, multi-stranded cables are seen as a better option than a large single strand. It is common practice to transpose the strands in a multi-strand wire so that each strand occupies the same average position as every other

strand [12]. The losses in the multi-stranded wire were simulated and analyzed. The 3-strand coil was modeled with a gap of 0.1 mm between each wire. It can be seen in Fig. 2 there is a gap between the wire stands due to the braiding process and this gap was used to represent the estimated average gap between each wire strand. Fig. 8 (b) presents the current distribution in the 3 strands. Although the current is still shared equally in the 3 strands, the distribution of current within each conductor has itself been changed. This is caused by the electromagnetic proximity effect and it results in the current being re-distributed towards the outer edge of the superconducting core. The maximum current density for a single wire carrying the same current was found to be 730 A/mm^2 and it is clear from Fig. 8 (b) that the redistribution of the current in the MgB$_2$ due to the proximity effect, has increased the maximum current density to 754 A/mm^2. This localized increase in the current density within the superconductor therefore could lead to an overall quench current for the 3-strand wire which is slightly lower than the expected design value of 3 times the quench current for a single wire. The loss in each strand of this 3-strand coil was found to be approximately 1.4 times that for a single stand.

Increasing the number of strands from 3 to 9 for example, introduces a further problem because the total current in each strand may no longer share equally. The current in each strand depends on the coil twist pitch and frequency. The modeling for both worst and best case scenarios was considered. In the worst case scenario, the current can be distributed freely in the strands if the twist pitch is too long or it is not properly twisted. As shown in Fig. 8 (c), it is clear that the middle strand carries almost no current. Any unequal current distribution is a key design issue because the total critical current for the multi-stranded cable will be reduced if the current is not shared equally. The maximum current density in the 9-strand wire has further increased to 803 A/mm^2; 10% higher than the value in the single wire. Considering *E-J* power law with an *n*-value of 30, a 10% increase in the current density in a small area of the superconductor can lead to increase in the AC losses on that area by a factor of 17. The average loss here in each strand of the 9-strand coil is a factor of 3.1 times that for a single strand. In the best case scenario, each strand carries the same average current but the current can also redistribute itself in the strand due to the proximity effect even if the twist pitch is properly designed. The increased losses are caused by this uneven current distribution in the multi-stranded wire. Fig. 8 (d) shows that the maximum current density in the properly transposed 9-strand wire has reduced from 803 A/mm^2 to 776 A/mm^2. The proximity effect however has still caused an increase in the maximum current density in the wire strands compared to a single wire. The model also showed that by correctly transposing the strands, the average loss in each strand was reduced to a factor of 2.5 times that for a single stand. Similar experimental and simulation results have been observed in YBCO Roebel cables [13, 14].

Transposing the multi-strand wire with a properly designed twist pitch therefore helps to reduce the AC losses and ensure

each strand carries the same average current. The FE results suggest that the benefits gained using multi-stranded MgB$_2$ wire to increase the current capacity and reduce AC losses may not be as high as the Norris model predict due to the proximity effect. The FE models also confirmed the issues of reduced quench current density and increased losses as the number of strands increase highlighted by the experimental testing.

(a) Single strand

(b) 3 strands

(c) 9 strands – worst case scenario

(d) 9 strands – best case scenario
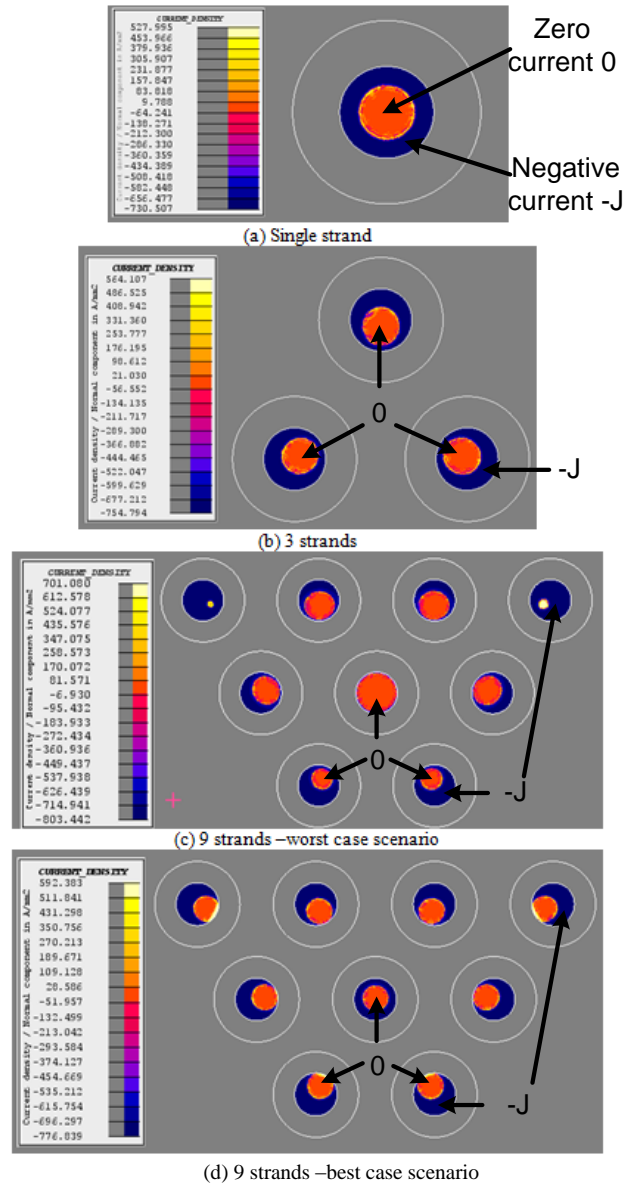
Fig. 8. Current density distribution at 0.015 second (system frequency of 50 Hz)

V. CONCLUSION

A monofilament 0.36 mm MgB$_2$ wire using a stainless steel sheath was used to build three SFCL coils with 3 strands, 16 strands and 50 strands of the MgB$_2$ wire. The experimental results showed the measured quench current densities reduced as the strand number increased and the AC losses increased as the strand number increased.

The multi-strand wire FE model shows that the proximity effect can lead to a very uneven current distribution in the

multiple strands reducing the overall current capacity and an increase in the AC losses. The FE models confirmed the issues of reduced quench current density and increased losses as the number of strands increase highlighted by the experimental testing.

Transposing the multi-stranded wire so that each strand occupies the same average wire position as every other strand along the length of the wire is shown be to an option for practical design.

REFERENCES

[1] L. Ye, et al., "Experimental studies of the quench behaviour of MgB$_2$ superconducting wires for fault current limiter applications," *Supercond. Sci. and Technol.*, vol. 20, pp. 621-628, Jul. 2007.

[2] L. Ye, et al., "Investigations of current limiting properties of the MgB$_2$ wires subjected to pulse overcurrents in the benchtop tester," *Supercond. Sci. and Technol.*, vol. 20, pp. 320-326, Apr. 2007.

[3] A. Oliver, A. C. Smith, M. Husband, M. Bailey, and Y. Feng, "Assessment of small bend diameter magnesium diboride wire for a superconducting fault current limiter application," *IEEE Trans. Appl. Supercond.,* vol. 19, pp. 1942-1945, Jun. 2009.

[4] X. Pei, A. C. Smith, M. Husband, and M. Rindfleisch, "Experimental tests on a superconducting fault current limiter using three-strand MgB$_2$ wire," *IEEE Trans. Appl. Supercond.,* vol. 22, Jun. 2012, Art. ID. 5600405.

[5] A. C. Smith, A. Oliver, X. Pei, M. Husband, and M. Rindfleisch, "Experimental testing and modelling of a resistive type superconducting fault current limiter using MgB$_2$ wire," *Supercond. Sci. and Technol.*, vol. 25, Dec. 2012, Art. ID. 125018.

[6] X. Pei, X. Zeng, A. C. Smith, and D. Malkin, "Resistive superconducting fault current limiter coil design using multistrand MgB$_2$ wire," *IEEE Trans. Appl. Supercond.,* vol. 25, Jun. 2015 Art. ID. 5602105.

[7] L. Martini, M. Bocchi, M. Ascade, A. Valzasina, V. Rossi, G. Angeli, and C. Ravetta, "Development, testing and installation of a superconducting fault current limiter for medium voltage distribution networks," *Physics Procedia*, Vol. 36, pp. 914-920, 2012.

[8] F. Grilli, et al., "Computation of losses in HTS under the action of varying magnetic fields and currents," *IEEE Trans. Appl. Supercond.,* Vol. 24, pp.78-110, 2014.

[9] X. Pei, A. C. Smith, X. Zeng, M. Husband, and M. Rindfleisch, "Design, build and test of an AC coil using MgB$_2$ wire for use in a superconducting machine," *IEEE Trans. Appl. Supercond.,* Vol. 23, Jun. 2013, Art. ID. 5202605.

[10] W. Norris; "Calculation of hysteresis losses in hard superconductors carrying AC: Isolated conductors and edges of thin sheets" J. Phys. D, Appl. Phys., Vol. 3, pp. 489-507, 1970.

[11] S. Stavrev, "Modelling of high temperature superconductors for AC power application", Lausanne, 2002.

[12] M. D. Sumption, P. N. Barnes, E. W. Collings, "AC losses of coated conductors in perpendicular fields and concepts for twisting," *IEEE Trans. Appl. Supercond.,* Vol. 15, pp. 2815-2818, 2005.

[13] Z. Jiang, et al., "Transport AC loss characteristics of a nine strand YBCO Roebel cable," *Supercond. Sci. and Technol.*, Vol. 23, Jan. 2010 Art. ID. 025028.

[14] F. Grilli and E. Pardo, "Simulation of ac loss in Roebel coated conductor cables", *Supercond. Sci. and Technol.*, Vol. 23, Oct. 2010, Art. ID. 115018.